

Effect of mechanical force on domain switching in BiFeO₃ ultrathin films

[ShiLu Tian](#), [Can Wang](#), [Yong Zhou](#), [Yu Feng](#), [XiaoKang Yao](#), [Chen Ge](#), [Meng He](#), [GuoZhen Yang](#) and [KuiJuan Jin](#)

Citation: *SCIENCE CHINA Physics, Mechanics & Astronomy* **63**, 217711 (2020); doi: 10.1007/s11433-019-9415-9

View online: <http://engine.scichina.com/doi/10.1007/s11433-019-9415-9>

View Table of Contents: <http://engine.scichina.com/publisher/scp/journal/SCPMA/63/1>

Published by the [Science China Press](#)

Articles you may be interested in

[Effect of induced shielding current transmission in longitudinal direction on levitation force of melt grown single-domain YBa₂Cu₃O_{7-x} cylindrical superconductor](#)

Science in China Series G-Physics, Mechanics & Astronomy **47**, 146 (2004);

[Epitaxial growth of ultrathin ZrO₂\(111\) films on Pt\(111\)](#)

Chinese Science Bulletin **56**, 502 (2011);

[The effect of oxide Bi₂O₃ doping on the levitation force of single domain YBCO bulk superconductors](#)

SCIENTIA SINICA Physica, Mechanica & Astronomica **42**, 346 (2012);

[Effect of HfO_x buffer layer on the resistive switching characteristics of γ-Fe₂O₃ nanoparticle films](#)

SCIENTIA SINICA Physica, Mechanica & Astronomica **44**, 417 (2014);

[Effect of thickness on structures of ultrathin diamond-like carbon films](#)

Chinese Science Bulletin **55**, 1949 (2010);

Effect of mechanical force on domain switching in BiFeO₃ ultrathin films

ShiLu Tian^{1,2}, Can Wang^{1,2,3*}, Yong Zhou¹, Yu Feng¹, XiaoKang Yao¹, Chen Ge¹,
Meng He¹, GuoZhen Yang¹, and KuiJuan Jin^{1,2,3*}

¹ *Institute of Physics, Chinese Academy of Sciences, Beijing 100190, China;*

² *University of Chinese Academy of Sciences, Beijing 100049, China;*

³ *Songshan Lake Materials Laboratory, Dongguan 523808, China*

Received February 28, 2019; accepted April 22, 2019; published online July 17, 2019

Ferroelectric polarization can be switched by an external applied electric field and may also be reversed by a mechanical force via flexoelectricity from the strain gradient. In this study, we report the mechanical writing of an epitaxial BiFeO₃ (BFO) thin film and the combined action of an applied mechanical force and electric field on domain switching, where the mechanical force and electric field are applied using the tip of atomic force microscopy. When the applied force exceeds the threshold value, the upward polarization of the BFO thin film can be reversed by pure mechanical force via flexoelectricity; when an electric field is simultaneously applied, the mechanical force can reduce the coercive electric field because both the piezoelectricity from the homogeneous strain and the flexoelectricity from strain gradient contribute to the internal electric field in the film. The mechanically switched domains exhibit a slightly lower surface potential when compared with that exhibited by the electrically switched domains due to no charge injection in the mechanical method. Furthermore, both the mechanically and electrically switched domains exhibit a tunneling electroresistance in the BFO ferroelectric tunnel junction.

BFO, flexoelectricity, mechanical writing, ferroelectric domain reversal

PACS number(s): 68.37.Ps, 77.80.Fm, 77.84.-s, 84.37.+q

Citation: S. L. Tian, C. Wang, Y. Zhou, Y. Feng, X. K. Yao, C. Ge, M. He, G. Z. Yang, and K. J. Jin, Effect of mechanical force on domain switching in BiFeO₃ ultrathin films, *Sci. China-Phys. Mech. Astron.* **63**, 217711 (2020), <https://doi.org/10.1007/s11433-019-9415-9>

1 Introduction

Conventional piezoelectricity describes the coupling between the electric polarization and the strain existing only in non-centrosymmetric materials, whereas flexoelectricity describes the coupling between the electric polarization and the strain gradient in all the insulators. In 1964, Kogan [1] theoretically predicted the flexoelectric effect; Bursian and Zaikovskii [2] experimentally confirmed it four years later,

and this effect was introduced as flexoelectricity by Indenbom et al. [3] in 1981. However, when compared with the extensively researched phenomena of piezoelectricity and ferroelectricity [4,5], flexoelectricity has been much less thoroughly investigated because the flexoelectric effect was negligibly weak in the solid bulk materials. Therefore, researchers have diverted their attention to flexoelectricity in thin films, where huge strain gradients (6-7 orders of magnitude larger than those in the corresponding bulk materials) [6,7] have been induced through controlled film growth in recent years [8-10]. More interestingly, ferroelectric materials exhibit large flexoelectric coefficients, which make the

*Corresponding authors (Can Wang, email: canwang@iphy.ac.cn; KuiJuan Jin, email: kjjin@iphy.ac.cn)

induced flexoelectricity sufficiently strong to interact with the as-grown ferroelectric polarization [11].

In ferroelectrics, if the external electric, piezoelectric, and flexoelectric contributions are considered, the polarization response (P_i) can be written as [12,13]:

$$P_i = \varepsilon_0 \chi_{ij} E_j + e_{ijk} u_{jk} + \mu_{ijkl} \frac{\partial u_{kl}}{\partial x_j}, \quad (1)$$

where the three terms on the right-hand side refer to the dielectric response, piezoelectric response, and flexoelectric response, respectively, ε_0 denotes the vacuum permittivity, χ denotes the dielectric susceptibility, E denotes the electric field strength, u denotes the strain, e denotes the piezoelectric polarization coefficient, and μ denotes the flexoelectric polarization coefficient. This equation indicates that the polarization in ferroelectrics varies with the strain and the strain gradient induced by an applied force.

With advances in thin-film fabrication methods, the internally-induced flexoelectric effect has been explored to influence the as-grown polarization by intrinsic factors such as the oxygen vacancy [7], deposition temperature [14], and lattice mismatch with substrates [15]. However, an exogenous flexoelectric effect could be more valuable, and researchers have explored mechanical polarization switching by pressing an atomic force microscope tip onto ferroelectric thin films such as BaTiO₃ [16,17] and PbZr_{0.2}Ti_{0.8}O₃ (PZT) [18]. However, the mechanical writing on the multiferroic BiFeO₃ (BFO) thin films has seldom been reported [19,20] because of its relatively high coercive field. The BFO thin films simultaneously show strong ferroelectric and weak magnetic properties at room temperature [21,22]; thus, we obtain promising functional features, enabling their use in switchable diodes [23-25] and ferroelectric tunnel junctions [26,27], as well as interesting photovoltaic effects [28-30] and magnetoelectric effects [31].

In general, the homogeneous applied stress can vary the polarization of materials via the piezoelectric effect or ferroelastic domain switching [32,33]. In this study, the mechanical switching of the ferroelectric polarization in a BFO epitaxial thin film was investigated using the tip of an atomic force microscope, which can induce large strain and strain gradient in the thin film. Additionally, the combined action of an applied mechanical force and applied electric field on the domain switching was explored.

2 Experimental details

A 10 nm-thick BFO thin film was grown on La_{0.67}Sr_{0.33}MnO₃ (LSMO)-coated 001-oriented SrTiO₃ (STO) single crystal substrates using a laser molecular beam epitaxy system. The STO substrates were etched with buffered hydrofluoric acid (HF) to eliminate the SrO layer and obtain a surface terminated only with TiO₂ [34]. Before the deposition of the BFO

thin film, a 20 nm-thick LSMO layer was grown on the STO substrates as a bottom electrode for the subsequent electric characterizations. Thin films were grown using an XeCl excimer laser with a wavelength of 308 nm, an energy density of approximately 1.5 J/cm², and a repetition rate of 2 Hz. During growth, the substrate was maintained at 640°C for BFO and at 800°C for LSMO; further, the oxygen pressure in the chamber was maintained at 15 Pa.

Piezoreponse force microscope (PFM) and scanning Kelvin probe force microscope (SKPFM) were conducted using a commercial atomic force microscope (MFP-3D, Asylum Research) equipped with a Ti/Ir-coated Si tip with a radius of 25 nm and a spring constant of 42 kN/m. Conductive atomic force microscope (C-AFM) was performed using a Pt/Ir-coated Si tip; the voltage was applied to the bottom electrode for C-AFM mode. More details of the growth methods and the characterization of the basic properties are available elsewhere [35].

3 Results and discussion

The high crystallinity of the (001) epitaxial BFO/LSMO/STO thin film without any impurity phase was verified by X-ray diffraction patterns (not shown here). PFM was used for mechanical writing and electrical writing and for characterizing the ferroelectric domains. Because of the extremely sharp tips, a huge strain and strain gradient can be created in the thin films by pressing the sharp tip against the sample surface. The typical tip force in the PFM contact mode was approximately 50 nN to ensure good contact between the tip and the sample surface. In conventional electrical writing, a positive or negative voltage that was greater than the coercive voltage was applied to the sample via the AFM tip to reverse the polarization, whereas in mechanical writing, a much greater force is loaded onto the tip to mechanically press against the sample in the absence of an applied voltage. The mechanically induced strain gradient coupling with the polarization via the flexoelectric effect can effectively modulate the intrinsic polarization.

Figure 1(a) depicts the mechanical polarization switching process with the application of a gradually increasing mechanical force to the as-grown upward-polarized BFO thin film (here, “upward” refers to the polarization direction pointing from the substrate to the surface (denoted as ⊙), whereas “downward” refers to the polarization from the surface to the substrate (denoted as ⊗)). When the force reaches 2000 nN, a reversed domain can be observed, and all the domains are switched to the downward state with increasing force when the force is greater than 3000 nN. Therefore, the threshold of the mechanical force for mechanical writing of the BFO thin film is approximately 2000 nN, and an AFM tip loaded with force greater than

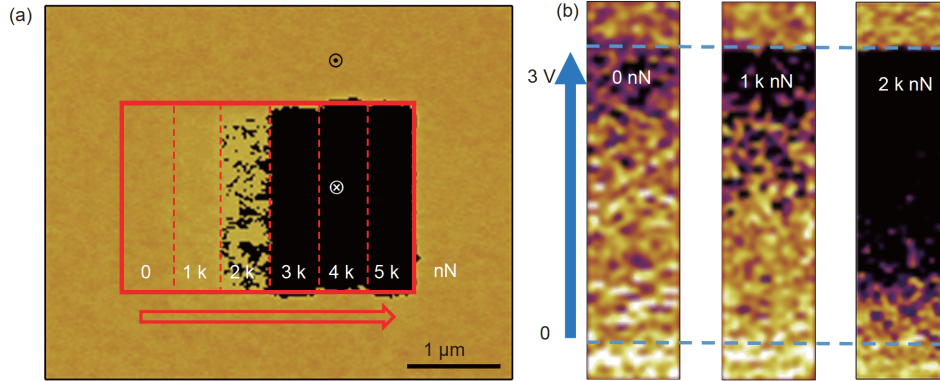


Figure 1 (Color online) PFM phase images of domain reversal by increasing the mechanical force from 0 to 5000 nN in increments of 1000 nN (a) and simultaneously increasing the force from 0 to 2000 nN and increasing the electric voltage from 0 to 3 V (b).

2000 nN can effectively reverse the ferroelectric domain from upward to downward. To probe the combined effects of the electrical and mechanical methods, an electrical voltage and mechanical force were simultaneously applied to the film. As illustrated in Figure 1(b), the electric coercive voltage decreases with increasing applied mechanical force and vice versa, confirming the combined effect of the mechanical force and electric field to switch the polarization from upward to downward.

To further investigate the effect of the mechanical force on the coercive voltage, we recorded the PFM switching loops of the thin film when an additional mechanical force was simultaneously applied. Figure 2 depicts the phase and amplitude loops acquired under various mechanical forces ranging from 0 to 1000 nN. The square phase hysteresis loop switching is approximately 180° , which illustrates complete bipolar reversal. The phase loop measured at zero additional mechanical force is shifted slightly toward the positive voltage side, indicating an upward built-in electric field, which is consistent with the as-grown upward polarization states of the BFO thin films. Furthermore, the positive coercive voltage decreases with the increasing mechanical force, whereas the negative coercive voltage does not obviously change. Here, the positive switching represents the reversal of the polarization from the upward to the downward direction and the negative switching represents the reversal from downward to upward. The decreased positive coercive voltage, which is accompanied by an increase in the applied force, indicates that the observed positive switching can be attributed to the combined effect of the applied electric field and the mechanical force. The strain and the strain gradient in the thin film originating from the mechanical force applied by an AFM tip are likely to contribute to polarization switching via the piezoelectric effect and the flexoelectric effect, respectively, and the pressure stress may also contribute to polarization reversal through the ferroelastic domain switching [36].

Here, we focus on the internal electric field variation in-

duced by the flexoelectric and piezoelectric effects. The flexoelectric field, which refers to the internal electric field caused by the flexoelectric effect, can be estimated according to the following equation [7,14,16,37-40]:

$$E_{\text{flexo}} = \frac{\lambda q}{\varepsilon_0 a_j} \frac{\partial u_{jk}}{\partial x_i}, \quad (2)$$

where λ , q , ε_0 , and a denote the scaling factor, electronic charge, vacuum permittivity, and lattice constant, respectively. For perovskite oxides, the value of λ is in the order of 10^0 or 10^1 [11,14]; we used $\lambda=5$ for the BFO thin film. For a pressure of approximately 2 GPa (4000 nN applied by an AFM tip with a radius of 25 nm) applied to the sample and for an elastic modulus of BFO of approximately 200 GPa [41,42], we assume that the induced strain (1%) relaxes within 10 nm, so the strain gradient is $\sim 10^6 \text{ m}^{-1}$. Thus, the flexoelectric field can be estimated as 2.3 MV/cm, which is comparable to the coercive field of the BFO thin films.

The piezoelectric field, which represents the electric field caused by the piezoelectric effect, can be approximately estimated by

$$E_{\text{piezo}} = u_3 d_{33}^{-1}, \quad (3)$$

where the maximum strain u_3 is assumed to be 1% and d_{33} is the longitudinal inverse piezoelectric coefficient. The d_{33} of the BFO film, as obtained from the amplitude loops (recorded at frequency away from resonance), is approximately 50 pm/V, in agreement with the previously reported values [43]. As a result, the piezoelectric field can reach 2 MV/cm, indicating that the piezoelectric effect can make contribution in the polarization reversal process, and that the internal electric field arising from the piezoelectricity should also be taken into account to explain the observed asymmetric shift of the coercive field denoted in Figure 2.

Notably, although the piezoelectric effect cannot independently switch the polarization, the piezoelectric field certainly plays a role in the polarization switching process, especially in our ultrathin film. Therefore, both the piezo-

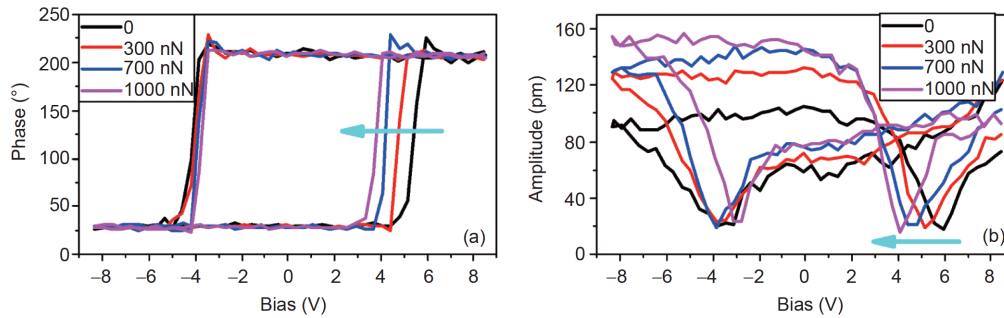


Figure 2 (Color online) The PFM switching loops of the BFO thin film recorded at frequency away from resonance under different mechanical forces. (a) Phase hysteresis loops; (b) amplitude butterfly loops.

electricity from the homogenous strain and the flexoelectricity from the strain gradient contribute to the internal electric field in the film; in addition, in the mechanical writing process, the piezoelectric effect can assist or resist the flexoelectric effect in ferroelectric polarization reversal. The polarization direction induced by the flexoelectric effect remains the same as the direction of the strain gradient; thus, the flexoelectric polarization always points from the surface of the film toward the substrate. In contrast, the piezoelectric coefficient has opposite signs for different polarization states [44], indicating that the piezoelectric field has different directions depending on the domain orientation. Thus, the piezoelectric effect positively contributes to both the positive switching and the negative switching. This view is consistent with the experimental results of Zhou et al. [45], who reported a reduction in the positive and negative coercive fields with increasing compressive stress in the PZT piezoceramic materials. However, the flexoelectric effect from the strain gradient induced by the tip press can only result in downward polarization. Consequently, for upward-polarized domains, the coaction of the flexoelectric effect and piezoelectric effect leads to a decrease in the positive coercive voltage. Because the flexoelectric field and piezoelectric field are of the same order of magnitude, their contributions to the positive switching in our samples are likely to be similar. Thus, the positive coercive voltages decrease gradually with the combination of flexoelectric and piezoelectric effects under increasing applied mechanical force. However, the flexoelectric effect and the piezoelectric effect have almost completely opposite contributions and counteract each other for negative switching; thus, no obvious shift can be observed in the negative coercive voltage, as depicted in Figure 2.

Figure 1(b) clearly denotes that the coercive voltage for electrical switching decreases with increasing mechanical force, confirming the equivalent effect of the electrically and mechanically downward polarization switching. The electrical reversibility of the mechanically written domain was also confirmed by successive mechanical and electrical writings in the same area. The electrical writing with a ne-

gative voltage on the tip effectively reversed the mechanically poled downward polarization to the upward state, whereas the positive voltage favored downward polarization. The mechanical force also switched the upward domain poled by electrical voltage to the downward state and had no effect on the downward domain. The mechanical and electrical writings were repeated and reversed, confirming that the mechanical writing method was effective and non-destructive in case of thin films. Notably, mechanical writing can also be achieved using an insulating tip, which further demonstrates the contribution of mechanical force in the absence of an external electric effect.

To compare the mechanical and electrical methods, we switched the ferroelectric polarization of two adjacent areas on the BFO thin film from upward to downward by applying mechanical force and electrical voltage, respectively. Mechanical writing was performed with an AFM tip loaded with 4000 nN and zero voltage, whereas +6 V was applied to the tip to conduct the electrical switching. The subsequent PFM measurement (Figure 3(b)) indicates that both the mechanical writing area marked with a red rectangle and the electrical writing area marked with a blue rectangle denote reversed downward polarization, demonstrating complete domain switching from upward to downward orientation in the BFO thin films by the application of the mechanical force and electrical voltage, respectively. The domains poled by mechanical and electrical methods have very similar PFM results, both of which have achieved reversal to downward polarization states. Thus, the effect of mechanical force to switch the polarization to downward states is equivalent to that of the external electrical field. To analyze the surface potential of the domains poled by the mechanical force and electric fields, the SKPFM [46] was used to detect the potential difference between the sample surfaces and the conductive tip, representing the charge distribution on the sample surface. Figure 3(c) and (d) denotes that the downward-switched domains exhibit a higher potential than that exhibited by the as-grown area and that the potential of the mechanically written domain is lower than that of the electrically switched domain. The high surface potential in-

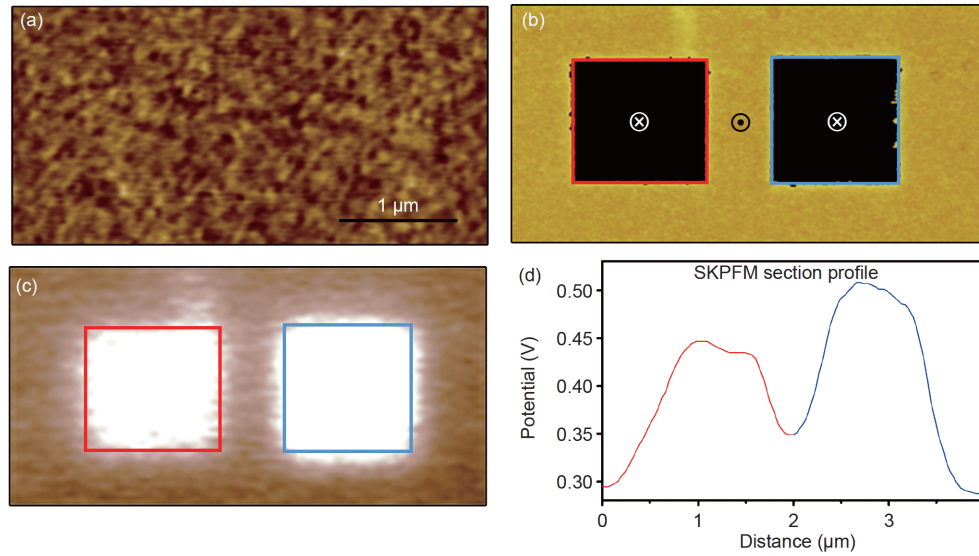


Figure 3 (Color online) The PFM and SKPFM images of the mechanically and electrically written domain. (a) Surface topography; (b) PFM phase; (c) SKPFM images; and (d) section profile across the SKPFM images. The size of the images is $4\ \mu\text{m} \times 2\ \mu\text{m}$ (the red rectangle denotes the mechanically written domain, whereas the blue one denotes the electrically written domain).

icates strong positive screen charges, and the surface potential is related to the remnant polarization and screen charges on the ferroelectric surface [46]. For the as-grown upward domains, the screen charges to neutralize the polarization charges mainly arise from the internal and ambient charges. During the polarization switching from upward to downward under an applied positive voltage, positive charges are over-injected from the conductive tip to accumulate on the surface. A portion of the injected charges screen the remnant polarization charges, and the other injected charges at the surface may be reduced with time by the recombination of the surface or ambient movable charges [47,48]. In this case, the injected positive charges on the electrically switched downward domain cause an increase in the surface potential. However, the surface charge of the mechanically switched domains only comprises internal charges and adsorbed ambient charges, which makes the surface potential slightly lower than that of the electrically switched domains. This result provides a new insight into the screen-charge formation mechanism during the ferroelectric polarization switching process.

Figure 4 demonstrates the ferroelectric tunneling electroresistance of the aforementioned mechanically and electrically poled downward domains and the as-grown upward domains of the BFO thin film by C-AFM. The current map obtained at a reading voltage of +1.5 V on the bottom electrode clearly shows that the downward-polarized domains exhibit higher conductivity than that exhibited by the as-grown upward domains, which is caused by a decrease in the average potential barrier height and thickness [27,49,50]. The top and bottom electrodes have different screening lengths, which lead to the asymmetry of the electrostatic

potential profile for opposite polarization directions. As shown in Figure 4(d), for the as-grown upward-polarized state, the potential at the BFO/LSMO interface is higher than that at the Pt/BFO interface, and the positive screening charges will aggregate at the bottom interface. Conversely, as the polarization reverses, the potential will increase at the top interface and decrease at the bottom interface, accompanied by the accumulation of negative screening charge at the bottom electrode. The LSMO bottom electrode has a larger screening length than that of Pt; thus, the decrease in the barrier height at the bottom interface is greater than the increase in the barrier height at the top interface when the polarization is switched from upward to downward. Therefore, the average barrier height decreases. In addition, the effective barrier thickness can also be adjusted by polarization switching. When polarization points downward, the negative screening charge in the bottom electrode bends the conduction band downward, reducing the barrier height. However, for upward polarization, the positive screening charge bends the band up, exceeding the Fermi energy and forming a space charge region in the bottom electrode which increases the effective barrier thickness. Furthermore, we observed similar conductance for the mechanically poled and electrically poled domains, which differs from the report of Lu et al. [17], who reported that the conductance of the mechanically poled domain was markedly larger than that of the electrically poled one in a BaTiO₃ thin film, which can be attributed to a lower screening charge density for the mechanically written domain. However, in our case of BiFeO₃ thin films, the SKPFM results denote comparable screening charges for the mechanically and electrically written domains, resulting in their similar electroresistance values.

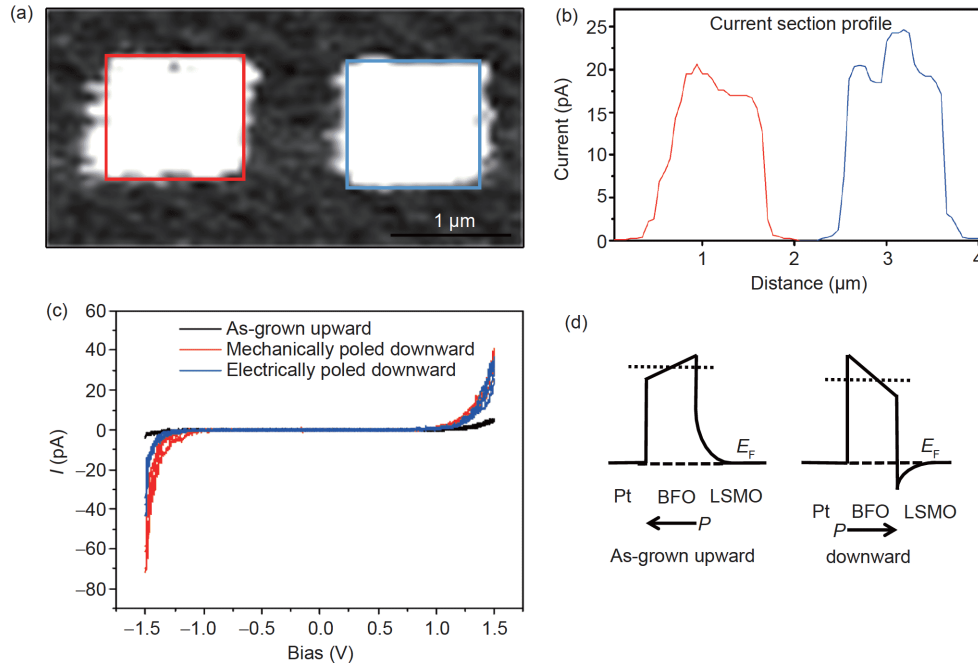


Figure 4 (Color online) Conductive-AFM measurements of the mechanically and electrically written domains of the BFO thin films. (a) Current map that was read at 1.5 V; (b) section profile of the current map; (c) local I - V curves obtained at different polarized domains; (d) band alignment schematic of the Pt/BFO/LSMO ferroelectric tunnel junctions. For the C-AFM measurements, the bias is applied at the bottom electrode; the red rectangle denotes the mechanically written domain, whereas the blue one denotes the electrically written domain.

4 Conclusions

In summary, we realized polarization reversal in the BFO epitaxial thin films with the mechanical force applied by the AFM tips in the absence of an applied external electric field via the flexoelectric effect. The involved flexoelectric and piezoelectric effects were quantitatively analyzed, and the combined action of an applied mechanical force and electric field on domain switching was clarified. The mechanically poled domains could also be reversed by an electric field, confirming the effectiveness of the mechanical writing method. Because of the lack of over-injected electrical charge, the mechanical writing domain exhibited a slightly lower surface potential when compared with that exhibited by the electrically poled domain, which lead to them exhibiting similar conductance values in the BiFeO₃ thin films. In addition, the flexoelectric effect is not exclusive to ferroelectrics; it exists in all the dielectric materials, indicating its extensive potential research value.

This work was supported by the National Key R&D Program of China (Grant No. 2017YFA0303604), the National Natural Science Foundation of China (Grant Nos. 11874412, 11674385, 11721404, and 11404380), and the Strategic Priority Research Program (B) of the Chinese Academy of Sciences (Grant No. XDB07030200).

1 S. M. Kogan, *Soviet Phys. Solid State* **5**, 2069 (1964).

2 E. V. Bursian, and O. I. Zaikovskii, *Soviet Phys. Solid State* **10**, 1121 (1968).

- 3 V. L. Indenbom, E. B. Loginov, and M. A. Osipov, *Kristallografiya* **26**, 1157 (1981).
- 4 A. Gruverman, and A. Kholkin, *Rep. Prog. Phys.* **69**, 2443 (2006).
- 5 J. F. Scott, *Science* **315**, 954 (2007).
- 6 D. Lee, and T. W. Noh, *Philos. Trans. R. Soc. A-Math. Phys. Eng. Sci.* **370**, 4944 (2012).
- 7 D. Lee, A. Yoon, S. Y. Jang, J. G. Yoon, J. S. Chung, M. Kim, J. F. Scott, and T. W. Noh, *Phys. Rev. Lett.* **107**, 057602 (2011), arXiv: [1106.3792](https://arxiv.org/abs/1106.3792).
- 8 K. J. Choi, M. Biegalski, Y. L. Li, A. Sharan, J. Schubert, R. Uecker, P. Reiche, Y. B. Chen, X. Q. Pan, V. Gopalan, L. Q. Chen, D. G. Schlom, and C. B. Eom, *Science* **306**, 1005 (2004).
- 9 I. Vrejoiu, G. Le Rhun, L. Pintilie, D. Hesse, M. Alexe, and U. Gösele, *Adv. Mater.* **18**, 1657 (2006).
- 10 Y. Feng, C. Wang, S. Tian, Y. Zhou, C. Ge, H. Guo, M. He, K. Jin, and G. Yang, *Nanotechnology* **27**, 355604 (2016).
- 11 W. Ma, *Phys. Stat. Sol. (B)* **245**, 761 (2008).
- 12 A. K. Tagantsev, *Phase Trans.* **35**, 119 (1991).
- 13 P. Zubko, G. Catalan, and A. K. Tagantsev, *Annu. Rev. Mater. Res.* **43**, 387 (2013).
- 14 B. C. Jeon, D. Lee, M. H. Lee, S. M. Yang, S. C. Chae, T. K. Song, S. D. Bu, J. S. Chung, J. G. Yoon, and T. W. Noh, *Adv. Mater.* **25**, 5643 (2013).
- 15 G. Catalan, A. Lubk, A. H. G. Vlooswijk, E. Snoeck, C. Magen, A. Janssens, G. Rispens, G. Rijnders, D. H. A. Blank, and B. Noheda, *Nat. Mater.* **10**, 963 (2011).
- 16 H. Lu, C. W. Bark, D. Esque de los Ojos, J. Alcalá, C. B. Eom, G. Catalan, and A. Gruverman, *Science* **336**, 59 (2012).
- 17 H. Lu, D. J. Kim, C. W. Bark, S. Ryu, C. B. Eom, E. Y. Tsymlal, and A. Gruverman, *Nano Lett.* **12**, 6289 (2012).
- 18 E. J. Guo, R. Roth, S. Das, and K. Dörr, *Appl. Phys. Lett.* **105**, 012903 (2014).
- 19 L. Chen, Z. Cheng, W. Xu, X. Meng, G. Yuan, J. Liu, and Z. Liu, *Sci. Rep.* **6**, 19092 (2016).
- 20 S. M. Park, B. Wang, S. Das, S. C. Chae, J. S. Chung, J. G. Yoon, L. Q. Chen, S. M. Yang, and T. W. Noh, *Nat. Nanotech.* **13**, 366 (2018).

- 21 Y. N. Venetsev, G. Zhdanov, and S. Solovev, *Soviet Phys. Crystallogr.* **4**, 538 (1960).
- 22 S. V. Kiselev, R. P. Ozerov, and G. S. Zhdanov, *Soviet Phys. Dokl.* **7**, 742 (1963).
- 23 A. Q. Jiang, C. Wang, K. J. Jin, X. B. Liu, J. F. Scott, C. S. Hwang, T. A. Tang, H. B. Lu, and G. Z. Yang, *Adv. Mater.* **23**, 1277 (2011).
- 24 C. Wang, K. Jin, Z. Xu, L. Wang, C. Ge, H. Lu, H. Guo, M. He, and G. Yang, *Appl. Phys. Lett.* **98**, 192901 (2011).
- 25 P. W. M. Blom, R. M. Wolf, J. F. M. Cillessen, and M. P. C. M. Krijn, *Phys. Rev. Lett.* **73**, 2107 (1994).
- 26 H. Yamada, V. Garcia, S. Fusil, S. Boyn, M. Marinova, A. Gloter, S. Xavier, J. Grollier, E. Jacquet, C. Carrétéro, C. Deranlot, M. Bibes, and A. Barthélémy, *ACS Nano* **7**, 5385 (2013).
- 27 A. Gruverman, D. Wu, H. Lu, Y. Wang, H. W. Jang, C. M. Folkman, M. Y. Zhuravlev, D. Felker, M. Rzechowski, C. B. Eom, and E. Y. Tsybal, *Nano Lett.* **9**, 3539 (2009), arXiv: 0906.1521.
- 28 S. Y. Yang, J. Seidel, S. J. Byrnes, P. Shafer, C. H. Yang, M. D. Rossell, P. Yu, Y. H. Chu, J. F. Scott, J. W. Ager, L. W. Martin, and R. Ramesh, *Nat. Nanotech.* **5**, 143 (2010).
- 29 W. Ji, K. Yao, and Y. C. Liang, *Adv. Mater.* **22**, 1763 (2010).
- 30 S. Y. Yang, L. W. Martin, S. J. Byrnes, T. E. Conry, S. R. Basu, D. Paran, L. Reichertz, J. Ihlefeld, C. Adamo, A. Melville, Y. H. Chu, C. H. Yang, J. L. Musfeldt, D. G. Schlom, J. W. Ager III, and R. Ramesh, *Appl. Phys. Lett.* **95**, 062909 (2009).
- 31 Y. H. Chu, L. W. Martin, M. B. Holcomb, M. Gajek, S. J. Han, Q. He, N. Balke, C. H. Yang, D. Lee, W. Hu, Q. Zhan, P. L. Yang, A. Fraile-Rodríguez, A. Scholl, S. X. Wang, and R. Ramesh, *Nat. Mater.* **7**, 478 (2008).
- 32 P. Gao, J. Britson, C. T. Nelson, J. R. Jokisaari, C. Duan, M. Trassin, S. H. Baek, H. Guo, L. Li, Y. Wang, Y. H. Chu, A. M. Minor, C. B. Eom, R. Ramesh, L. Q. Chen, and X. Pan, *Nat. Commun.* **5**, 3801 (2014).
- 33 J. Muñoz-Saldaña, G. A. Schneider, and L. M. Eng, *Surf. Sci.* **480**, L402 (2001).
- 34 G. Koster, B. L. Kropman, G. J. H. M. Rijnders, D. H. A. Blank, and H. Rogalla, *Appl. Phys. Lett.* **73**, 2920 (1998).
- 35 S. Tian, C. Wang, Y. Zhou, X. Li, P. Gao, J. Wang, Y. Feng, X. Yao, C. Ge, M. He, X. Bai, G. Yang, and K. Jin, *ACS Appl. Mater. Interfaces* **10**, 43792 (2018).
- 36 D. Edwards, S. Brewer, Y. Cao, S. Jesse, L. Q. Chen, S. V. Kalinin, A. Kumar, and N. Bassiri-Gharb, *Adv. Mater. Interfaces* **3**, 1500470 (2016).
- 37 A. K. Tagantsev, *Zhurnal Eksperiment. Teoretich. Fiziki* **88**, 2108 (1985).
- 38 W. Ma, and L. E. Cross, *Appl. Phys. Lett.* **81**, 3440 (2002).
- 39 R. Resta, *Phys. Rev. Lett.* **105**, 127601 (2010), arXiv: 1008.0837.
- 40 A. Gruverman, B. J. Rodriguez, A. I. Kingon, R. J. Nemanich, A. K. Tagantsev, J. S. Cross, and M. Tsukada, *Appl. Phys. Lett.* **83**, 728 (2003).
- 41 S. L. Shang, G. Sheng, Y. Wang, L. Q. Chen, and Z. K. Liu, *Phys. Rev. B* **80**, 052102 (2009).
- 42 H. Dong, C. Chen, S. Wang, W. Duan, and J. Li, *Appl. Phys. Lett.* **102**, 182905 (2013).
- 43 J. Wang, J. B. Neaton, H. Zheng, V. Nagarajan, S. B. Ogale, B. Liu, D. Viehland, V. Vaithyanathan, D. G. Schlom, U. V. Waghmare, N. A. Spaldin, K. M. Rabe, M. Wuttig, and R. Ramesh, *Science* **299**, 1719 (2003).
- 44 R. Holland, *IEEE Spectr.* **7**, 67 (1970).
- 45 D. Zhou, M. Kamlah, and D. Munz, *J. Eur. Ceramic Soc.* **25**, 425 (2005).
- 46 M. Rohwerder, and F. Turcu, *Electrochim. Acta* **53**, 290 (2007).
- 47 S. V. Kalinin, and D. A. Bonnell, *Phys. Rev. B* **63**, 125441 (2001).
- 48 L. Wang, K. J. Jin, J. X. Gu, C. Ma, X. He, J. Zhang, C. Wang, Y. Feng, Q. Wan, J. A. Shi, L. Gu, M. He, H. B. Lu, and G. Z. Yang, *Sci. Rep.* **4**, 6980 (2014).
- 49 M. Y. Zhuravlev, R. F. Sabirianov, S. S. Jaswal, and E. Y. Tsybal, *Phys. Rev. Lett.* **94**, 246802 (2005).
- 50 E. Y. Tsybal, and A. Gruverman, *Nat. Mater.* **12**, 602 (2013).